α-Emitters for Radiotherapy: From Basic Radiochemistry to Clinical Studies—Part 1

Sophie Poty[1], Lynn C. Francesconi[2,3], Michael R. McDevitt[1,4], Michael J. Morris[5], and Jason S. Lewis[1,6]

[1]Department of Radiology and Program in Molecular Pharmacology, Memorial Sloan Kettering Cancer Center, New York, New York; [2]Department of Chemistry, Hunter College, New York, New York; [3]Graduate Center of City University of New York, New York, New York; [4]Department of Radiology, Weill Cornell Medical College, New York, New York; [5]Department of Medicine, Memorial Sloan Kettering Cancer Center, New York, New York; and [6]Departments of Radiology and Pharmacology, Weill Cornell Medical College, New York, New York

Learning Objectives: On successful completion of this activity, participants should be able to (1) cite α-emitter families available for therapeutic use and understand their current production limit; (2) consider radiation safety concerns when handling α-emitters; and (3) overcome radiolabeling and daughter redistribution hurdles with the approaches described in this educational review.

Financial Disclosure: This work is supported by the Radiochemistry and Molecular Imaging Probe Core, which is supported in part by NIH/NCI Cancer Center Support Grant P30 CA008748. Jason Lewis is supported by the Mr. William H. and Mrs. Alice Goodwin and the Commonwealth Foundation for Cancer Research and by the Center for Experimental Therapeutics of Memorial Sloan Kettering Cancer Center. Sophie Poty is supported by the François Wallace Monahan Fellowship from the JLM Benevolent Fund. The authors of this article have indicated no other relevant relationships that could be perceived as a real or apparent conflict of interest.

CME Credit: SNMMI is accredited by the Accreditation Council for Continuing Medical Education (ACCME) to sponsor continuing education for physicians. SNMMI designates each *JNM* continuing education article for a maximum of 2.0 AMA PRA Category 1 Credits. Physicians should claim only credit commensurate with the extent of their participation in the activity. For CE credit, SAM, and other credit types, participants can access this activity through the SNMMI website (http://www.snmmilearningcenter.org) through June 2021.

With a short particle range and high linear energy transfer, α-emitting radionuclides demonstrate high cell-killing efficiencies. Even with the existence of numerous radionuclides that decay by α-particle emission, only a few of these can reasonably be exploited for therapeutic purposes. Factors including radioisotope availability and physical characteristics (e.g., half-life) can limit their widespread dissemination. The first part of this review will explore the diversity, basic radiochemistry, restrictions, and hurdles of α-emitters.

Key Words: radiotherapy; α-emitters; radiochemistry; clinical trials

J Nucl Med 2018; 59:878–884
DOI: 10.2967/jnumed.116.186338

Radionuclide strategies for curative therapy, disease control, or palliation are positioned to constitute a major portion of nuclear medicine. The range of available therapeutic radioisotopes, including α, β, or Auger electron emission, has considerably expanded over the last century (*1*). Matching the particle decay pathway, effective range, and relative biological effectiveness to tumor mass, size, radiosensitivity, and heterogeneity is the primary consideration for maximizing therapeutic efficacy. β-emitting radioisotopes have the longest particle pathlength (≤12 mm) and lowest linear energy transfer (LET) (~0.2 keV/μm), supporting their effectiveness in medium to large tumors (Fig. 1). Although the long β-particle range is advantageous in evenly distributing radiation dose in heterogeneous tumors, it can also result in the irradiation of healthy tissue surrounding the tumor site. Conversely, Auger electrons have high LET (4–26 keV/μm) but a limited pathlength of 2–500 nm that restricts their efficacy to single cells, thus requiring the radionuclide to cross the cell membrane and reach the nucleus. Finally, α-particles have a moderate pathlength (50–100 μm) and high LET (80 keV/μm) that render them especially suitable for small neoplasms or micrometastases. A recent clinical study highlighted the ability of α-radiotherapy to overcome treatment resistance to β-particle therapy, prompting a paradigm shift in the approach toward radionuclide therapy (*2*).

For optimized therapeutic efficacy, the α-cytotoxic payload is expected to accumulate selectively in diseased tissue and deliver a sufficient radiation dose to tumor sites while sparing normal organs and surrounding healthy tissue. Some α-emitting radionuclides (e.g., radium dichloride) demonstrate intrinsic bone-targeting properties, but most radionuclides require conjugation to carrier molecules for specific delivery to tumor cells. Targeted α-therapy relies on the significant differential targeting properties of a molecular vector in delivering the lethal α-payload to cells expressing higher target concentrations. Consequently, α-emitting radionuclides have been conjugated to a wide range of biomolecules, antibodies, peptides, small-molecule inhibitors, and nanocarriers. Numerous α-conjugates showing promising preclinical outcomes are now being evaluated in clinical trials or salvage therapy studies.

α-EMITTING ISOTOPE RADIOCHEMISTRY

The α-particle is a naked ^{4}He nucleus with a +2 charge; its extreme mass compared with that of electrons suppresses deflection of the particle, and its track is almost linear. α-particles are monoenergetic, with initial kinetic energy of between 5 and 9 MeV, yielding a corresponding particle range of 50–100 μm

Received Aug. 4, 2017; revision accepted Feb. 3, 2018.
For correspondence or reprints contact: Jason S. Lewis, Memorial Sloan Kettering Cancer Center, 1275 York Ave., New York, NY 10065.
E-mail: lewisj2@mskcc.org
Published online Mar. 15, 2018.

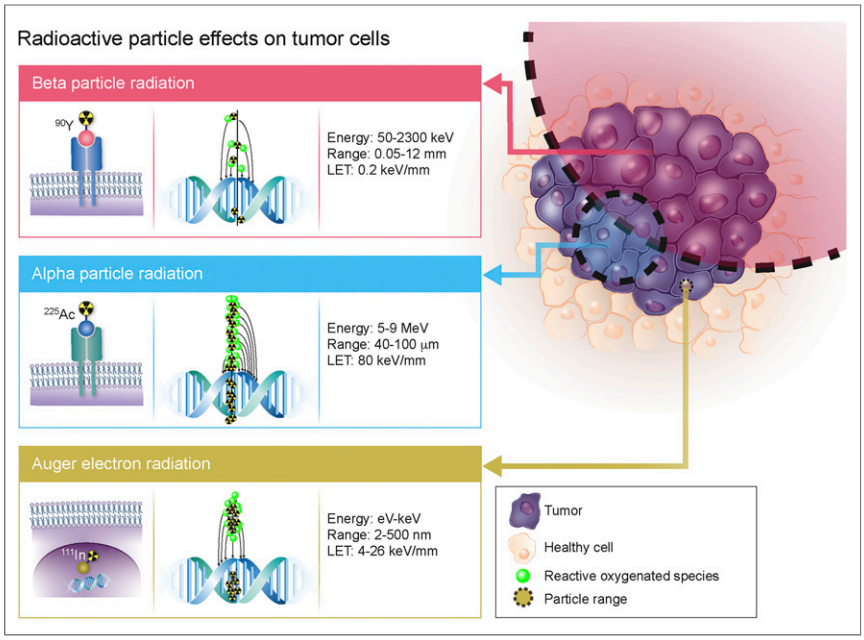

FIGURE 1. Comparison of therapeutic particle energies, particle ranges, LET, and DNA damage potencies.

(Fig. 1). α-particles are effective ionizing agents and are classified as high LET. Because α-particles cannot be directly imaged in vivo, the γ-photons, characteristic x-rays, or bremsstrahlung radiation that accompany decay of the parent radionuclide are often used for quantifying target uptake, dosimetry, and therapy response.

Complex molecular pathways are initiated when α-particles interact with biologic tissue (*3*). The primary target of high-LET radiation is DNA, and a single α-particle track can result in irreparable double-strand breaks (*4*). Nucleus traversal by α-tracks correlates with cytotoxicity, whereas traversal through the cytoplasm results in more moderate radiation-induced effects (*4,5*). In contrast, β-particle irradiation produces mainly single-strand breaks, exhibiting approximately 500 times lower cytotoxic potency than α-particles (Fig. 1) (*3*). The cross-fire effect is the ability of a particle to induce damage to multiple neighboring cells, offering an advantage in heterogeneous tumors (Fig. 2). Because of the particle range, this cross-fire effect is thought to be higher with β-emitters, but recent studies showing α-particles to have a significant therapeutic effect on large tumors question this concept (*6–8*). In addition to direct effects, indirect radiation effects have been observed. The radiation-induced bystander effect—DNA damage in cells surrounding irradiated cells but not directly exposed to radiation—also contributes to the impact of α-radiation (*6*). The mechanism of this effect is not fully understood but is hypothesized to result from extracellular reactive oxygenated species, chromosomal instabilities, or other abnormalities. Finally, the abscopal effect, resulting from a radiation-induced immune response, is characterized by a therapeutic response in remote lesions (*9*). Importantly, compared with β-particle radiotherapy, which relies mainly on the formation of reactive oxygen species, the cell-killing efficiency of α-particles was shown to be independent of cellular oxygenation (*10*).

Because of the different types of biologic damage caused by high and low LET, one should consider the relative biological effectiveness factor when performing dosimetry calculations so that the estimated absorbed dose reflects the probability and relative severity of a biological effect (*11*). Based on in vitro experiments, if the chosen endpoint is deterministic (e.g., therapeutic efficacy or toxicity), the relative biological effectiveness ranges from 3 to 7 and should be used when predicting the benefit of α-therapy. If the endpoint is stochastic, such as cancer induction, the relative biological effectiveness for α-particles is approximately 20 (*11*). Human experience, however, has indicated lower toxicity than expected and highlights the dire need to develop accurate dosimetry measurement techniques for α-emitters.

α-emitting radionuclides with potential applications for radiotherapy are presented below. Because most α-emitters are progeny in a common decay chain (or family)—either direct progeny or separated by short-half-life ($t_{½}$) radioactive intermediates—we elected to present radioisotopes of the same family together. Radioactive decay through multiple radioactive progeny is referred to as the in vivo generator or nanogenerator approach (*12*). This approach offers the significant advantage of enhancing toxicity by delivering several cytotoxic radionuclides to the tumor but also conversely suffers from the major hurdle of progeny redistribution.

^{211}At

^{211}At can be cyclotron-produced by bombarding natural bismuth with a medium-energy α-particle beam (28–29.5 MeV) using the ^{209}Bi(α,2n)^{211}At reaction (*13*). Even though the production and purification of ^{211}At are inexpensive, the number of accelerators capable of generating a 28-MeV α-particle beam limits the availability of this isotope (*13*).

With a $t_{½}$ of 7.2 h, ^{211}At decays via a branched pathway to stable ^{207}Pb, emitting α-particles via 2 pathways (Table 1). ^{211}At emits K x-rays with its α-decay to ^{211}Po, allowing for sample counting and scintigraphic imaging of ^{211}At in vivo (*14*). Astatine belongs to the halogen family, and radiolabeling can be performed by adapting radioiodination chemistry (*15*). Tin precursors and prosthetic groups have been used to label small molecules, peptides, or antibodies (*15*). The carbon–astatine bond is relatively weak, and the release of free astatine can result in undesired toxicity (*16*). Similar to iodine, free astatine accumulates in the thyroid, stomach, and macrophage-bearing organs such as the spleen and lung.

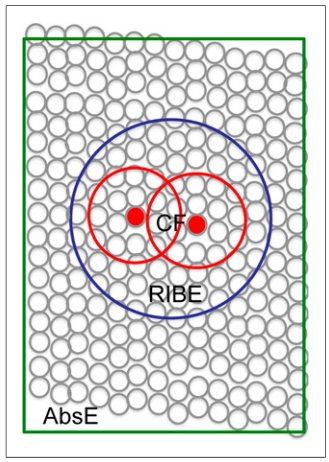

FIGURE 2. Indirect mechanisms increasing α-particle lethal potency, including cross-fire effect (CF), radiation-induced bystander effect (RIBE), and abscopal effect (AbsE) (*6*).

TABLE 1
α-Emitters for Radiotherapy, Together with Their Decay Progeny

Parent	Daughters	$t_{½}$	α-decay	α-energy (MeV)	Other emission	Radiochemistry	Free isotope accumulation	Study
^{211}At*		7.2 h	42%	5.87		Tin precursor, prosthetic group	Thyroid, stomach, spleen, lung	(*15*)
	^{211}Po	0.52 s	100%	7.45	Kα x-rays (77–92 keV)			
	^{207}Bi	38 y			100% electron capture			
	^{207}Po	Stable						
^{225}Ac*		9.9 d	100%	5.94		DOTA, DO3A chelator	Liver, bone	(*21,56*)
	^{221}Fr†	4.9 m	100%	6.45	218 keV γ		Kidneys, urine	
	^{217}At	32.3 ms	>99.9%	7.20				
	^{213}Bi*†	45.6 m	2.2%	5.87	492 keV β^- (97.8%); 440 keV γ	CHX-A″-DTPA, DOTA, NETA	Kidneys, urine	(*50*)
	^{213}Po	3.72 μs	100%	8.38				
	^{209}Tl	2.16 m			660 keV β^- (100%)			
	^{209}Pb	3.23 h			198 keV β^- (100%)			
	^{209}Bi	Stable						
^{227}Th*		18.7 d	100%	6.14	50 and 236 keV γ	DOTA, Me-3, 2-HOPO	Bone surface	(*25*)
	^{223}Ra*	11.4 d	100%	5.71	269 keV γ		Bone surface	(*57*)
	^{219}Rn	3.96 s	100%	6.82	271 keV γ			
	^{215}Po	1.78 ms	>99.9%	7.39				
	^{211}Pb†	36.1 m			471 keV β^- (100%); 404 keV γ		Blood, liver, skeleton, kidneys	(*58*)
	^{211}Bi†	2.14 m	99.7%	6.62	172 keV β^- (0.3%); 351 keV γ		Kidneys, urine	(*58*)
	^{207}Tl	4.77 m			492 keV β^- (100%)			
	^{207}Pb	Stable						
^{224}Ra*		3.63 d	100%	5.69	241 keV γ		Bone surface	(*30*)
	^{220}Rn†	55.6 s	100%	6.29				
	^{216}Po	0.15 s	100%	6.78				
	^{212}Pb*†	10.6 h			93.5 keV β^- (100%); 238 and 300 keV γ	TCMC	Blood, liver, skeleton, kidneys	(*31,32*)
	^{212}Bi*†	60.6 m	36%	6.05	834 keV β^- (64%); 727 and 1,620 keV γ	CHX-A″-DTPA, DOTA, NETA	Kidneys, urine	(*32*)
	^{212}Po	0.30 μs	100%	8.78				
	^{208}Tl	3.1 m			342, 441, 535, and 649 keV β^- (100%); 2,614 keV γ			
	^{208}Pb	Stable						

*α-emitters of interest.
†Daughters with redistribution potency.
DO3A = 2,2′,2″-(1,4,7,10-tetraazacyclododecane-1,4,7-triyl)triacetate.

^{225}Ac/^{213}Bi

The main source of ^{225}Ac is currently ^{229}Th generators ($t_{½}$ = 7.3 y), which can be milked over a 3-wk period and allow the separation of ^{225}Ra and ^{225}Ac (*17*). The Oak Ridge National Laboratory ^{299}Th generator produces up to 33.3 GBq per year. However, because of the limited number of generators worldwide, there is a severe shortage of this isotope for preclinical and clinical research. The ^{225}Ac shortage also inhibits ^{225}Ac/^{213}Bi generator manufacturing (*18*).

Possible pathways toward increasing ^{225}Ac production include high-energy proton spallation of ^{232}Th. A triinstitutional collaboration

among Oak Ridge, Brookhaven, and Los Alamos National Laboratories recently produced millicurie quantities of ^{225}Ac by irradiating a natural thorium target at beam energies of between 78 and 192 MeV (*19*). Using this method, a 10-d irradiation campaign of a 5 g/cm^2 thorium target was able to produce curie levels of ^{225}Ac (*19*). The quality of the accelerator-produced ^{225}Ac was equal to that of the ^{229}Th generated; however, the impact of coproduced ^{227}Ac remains to be evaluated (*19*).

^{225}Ac ($t_{½}$ = 10.0 d; 5.8-MeV α-particle) decays sequentially through 6 dominant daughters to stable ^{209}Bi (Table 1). Decay of a single ^{225}Ac atom yields 4 net α-disintegrations and 3 β-disintegrations together with the emission of 2 useful γ-emissions; it is therefore classified as a nanogenerator (*12*). The ^{225}Ac daughter ^{213}Bi ($t_{½}$ = 45.6 min; 97.8% β^-, 2.2% 6-MeV α-particle) is a widely studied radionuclide for targeted α-therapy in preclinical and clinical studies. ^{213}Bi forms stable complexes with nitrogen-rich chelators such as CHX-A″-DTPA (2-[*p*-isothiocyanatobenzyl]-cyclohexyldiethylenetriaminepentaaceticacid) or NETA ({4-[2-(bis-carboxymethylamino)-ethyl]-7-carboxymethyl-[1,4,7]triazonan-1-yl}-aceticacid), and both ^{213}Bi and ^{225}Ac are stable on coordination by the DOTA chelator (*20*). Free ^{225}Ac-acetate accumulates primarily in the liver and bone (percentage injected dose per gram: 111.8 ± 2.13 and 9.15 ± 1.2, respectively) (*21*). However, once chelated by DOTA, both liver uptake and bone uptake are significantly reduced (to 1.29 ± 0.25 and 0.98 ± 0.10, respectively) (*21*). The ^{225}Ac daughters ^{221}Fr and ^{213}Bi will preferentially accumulate in the kidneys and urine.

^{227}Th/^{223}Ra

^{227}Th and ^{223}Ra are both available on separation from their mutual parent, ^{227}Ac ($t_{½}$ = 21.7 d) (*22*). Clinical production of ^{223}Ra uses ^{227}Ac/^{227}Th-based generators (*23*). Parent isotopes are loaded on actinide chromatographic resin, and ^{223}Ra-chloride solution is obtained after elution with 1 M HCl or HNO_3, subsequent purification on a cation exchange column, evaporation, and dissolution in saline solution (*24*).

^{227}Th ($t_{½}$ = 18.7 d; 6.0-MeV α-particle) and its daughter, ^{223}Ra ($t_{½}$ = 11.4 d; 5.7-MeV α-particle), act as nanogenerators, releasing up to 4 high-energy α-particles before reaching stable ^{207}Pb (Table 1). Emission of γ-photons allows for scintigraphic imaging of both isotopes. Biodistribution of ^{227}Th-citrate indicates high uptake in the femur and parietal bone (*25*). ^{223}Ra is an alkaline earth metal similar to calcium that, like ^{227}Th, preferentially accumulates in sites of bone mineralization, binding into hydroxyapatite. γ-ray spectroscopy of the femur showed that, if released, ^{223}Ra redistributes to the bone because of the α-recoil energy, resulting in an increased dose to the bone surface (*25*). The lack of suitable chelating agents to coordinate ^{223}Ra limits the development of radioconjugates. On the other hand, ^{227}Th with its +4 oxidation state can be stably chelated by DOTA (*26*) and octadentate chelator with hydroxypyridinone coordinating moieties (e.g., *N*-methyl-3,2-hydroxypyridinone [Me-3,2-HOPO]) (*27*).

^{224}Ra/^{212}Bi

^{224}Ra, ^{212}Pb, and ^{212}Bi are produced by generators loaded with their long-lived parent, ^{228}Th (*28*). Severe radiolytic damage to the resin of the ^{228}Th-based generators was observed, and they were replaced by ^{224}Ra-based generators, from which ^{212}Bi and ^{212}Pb are obtained selectively (*29*).

^{224}Ra ($t_{½}$ = 3.6 d; 5.7-MeV α-particle; 241-keV γ-particle) decays into stable ^{208}Pb, producing 4 net α-particles and 2 β-particles, with the main recoil daughters being ^{212}Pb ($t_{½}$ = 10.6 h; 93.5-keV β^--particle) and ^{212}Bi ($t_{½}$ = 60.6 min; 36% 6.1-MeV α-particle) (Table 1). Because of its bone-seeking properties, ^{224}Ra was initially used to treat ankylosing spondylitis (*30*). Even though ^{212}Pb decays via a β-emission, its increased $t_{½}$, as compared with ^{212}Bi, allows for delivery of up to 10 times more dose per unit of administered activity, together with dose preparation and administration that are more routine. Although ^{212}Pb forms a stable complex with the DOTA chelator, acid-catalyzed dissociation was reported. The TCMC chelator (1,4,7,10-tetrakis(carbamoylmethyl)-1,4,7,10-tetraazacyclododecane) was later developed and demonstrated extremely high stability for the Pb(II) ion (*31*). During ^{212}Pb decay, γ-ray emissions compete with internal conversion over 30% of the time. The ejection of conversion electrons brings ^{212}Bi to highly ionized states (e.g., Bi^{5+} and Bi^{7+}), destabilizing the bismuth complexes and ultimately liberating the radionuclide (*32*). Although free ^{212}Pb accumulates in the blood, liver, bone, and kidneys, ^{212}Bi accumulates mainly in the kidneys and urine.

APPROACHES AND SPECIAL CONSIDERATIONS FOR HANDLING AND ADMINISTERING α-EMITTERS

Because an α-particle of at least 7.5 MeV is required to penetrate the protective skin layer (0.07 mm thick), pure α-emitters do not constitute an external radiation hazard. The main concern is internalization and energy deposition in healthy living tissues (*33*). Untoward radiation effects to humans from α-exposure include cancer induction, genetic diseases, teratogenesis, and degenerative changes; the respiratory tract, bone, liver, and reticuloendothelium system are the most important target tissues (*33*). The tumorigenesis potential of α-radiation was demonstrated after irradiation of human benign prostate epithelial cells in mice (*34*). Moreover, because of the bystander mutagenic effect, mutations and chromosomal aberrations have been observed in the DNA of cells that received no direct α-particle exposure, indicating that the current genotoxic risks of α-emitters are underestimated (*35*).

Proper handling of α-emitters is radionuclide-dependent, and each progeny must be considered because periodicity changes with decay. In the handling of α-emitters, special equipment to detect α-particles, such as ZnS(Ag) scintillators, should be available in addition to Geiger–Mueller survey meters (*36*). Allowable removable contamination levels for α-emitters are about 10 times lower (3.3 Bq/100 cm^2) than for β-emitting radionuclides. A well-ventilated hood or, ideally, a glove box should be used in the handling of α-emitters with low abundance and low-energy γ-emission. If highly energetic γ-rays are emitted during the radionuclide decay, all work should be performed in a shielded hot cell or behind 15-cm (6-in) lead bricks using manipulator arms or remote-handling conditions (*29*). Extra precautions, such as trapping or gas-tight enclosures, should be considered when volatile daughters such as radon are emitted. Double gloving is recommended. Wipe tests should be performed and monitored with a γ-counter and a liquid scintillation counter.

For clinical production, centralized production should be considered for isotopes of appropriate $t_{½}$. Radiochemists should be trained and have access to working and waste storage areas designed for a dedicated α-emitting isotope radiochemistry. Clinical doses should be prepared and injected once secular equilibrium is reached. Special considerations for $^{223}RaCl_2$ preparation, administration, and patient release were reported for a phase I clinical study to evaluate ascending doses of $^{223}RaCl_2$ at Memorial Sloan Kettering (*37*).

TARGETED α-THERAPY: VECTORS AND RADIOLABELING TECHNIQUES

Targeting moieties for targeted α-therapy include antibodies, peptides, or small molecules; each possesses advantages and pitfalls. Compared with small molecules, antibodies show favorable biodistribution, with high tumor uptake and low accumulation in healthy tissues. One notable example is prostate-specific membrane antigen small-molecule inhibitors (*2*); accumulation of these small-molecule drugs in the salivary glands is high, whereas the prostate-specific membrane antigen-specific antibody J591 shows low uptake (*38*). However, the longer blood circulation time of the antibody increases the risk of hemato- and myelotoxicity (*6*). On the other hand, small molecules and peptides exhibit higher tumor penetration and faster clearance (*6*). Because targeting moieties have a broad spectrum of pharmacokinetic profiles, it is important to match the physical $t_{½}$ of the therapeutic radionuclide to the biologic $t_{½}$ of the vector.

A radionuclide is conjugated to its vector using either a prosthetic group (^{211}At) or a chelate (^{227}Th, ^{225}Ac, ^{212}Pb, $^{213/212}$Bi). Vectors should be functionalized before the radiolabeling, and 1-step radiolabeling is preferred, especially with short-$t_{½}$ radionuclides. However, the development of α-particle radioimmunoconjugates may require more complex procedures. Radioastatination of antibodies is usually performed using a 2-step method in which an aromatic organotin precursor bearing an activated ester is radiolabeled and then conjugated to the antibody (*39*). Radiolabeling of DOTA conjugates with ^{225}Ac and ^{227}Th requires harsh conditions (high temperatures, pH extremes) that are not always compatible with sensitive biomolecules such as antibodies (*26*). McDevitt et al. developed a 2-step radiolabeling method in which an isothiocyanate C-functionalized derivative of the DOTA chelator is radiolabeled and then conjugated to the antibody at 37°C (*40*); however, this method suffers from low radiochemical yields (≤10%) because of hydrolysis of the isothiocyanate moiety. Maguire et al. later proposed a 1-step method for ^{225}Ac radiolabeling of monoclonal antibodies that allows for radiochemical yields of up to 80% (*41*). Other approaches imply the development of new chelators that form stable complexes at room temperature. Ramdahl et al. reported superior properties with respect to ^{227}Th radiolabeling and stability using Me-3,2-HOPO compared with the DOTA chelator (*27*).

Blood toxicity and normal-tissue irradiation, caused by the slow kinetic clearance of antibodies, led to the development of an alternate delivery approach called pretargeting, which separates administration of the targeting vector from that of the radioisotope (Fig. 3) (*42*). First, an unlabeled antibody that binds both an antigen and the radioligand is administered, accumulates in the tumor, and slowly clears from the blood and nontargeted tissues. A low-molecular-weight radioligand is subsequently administered and diffuses into the tumor, binding to the antigen-associated pretargeting conjugate. The rapid clearance of any excess radioligand results in improved tumor–to–normal-tissue ratios and lower radiation doses to healthy organs (*42*). Interaction between the pretargeted antibody and the radioligand uses the extraordinarily high affinity of avidin (or streptavidin) for biotin (*43*), bispecific antibodies (*44*), or bioorthogonal chemistry (*45*). This approach combines the advantages of antibodies (e.g., high targeting efficiency, penetration, long residence time) with those of small molecules (rapid clearance). Moreover, this technique allows the association of antibodies with short-$t_{½}$ radionuclides, such as ^{211}At (*46*) or $^{213/212}$Bi (*47*), increasing their therapeutic potential. Applicability and efficacy in humans, though, still need to be proven, and the antibody–antigen internalization should occur either through a slow process or not at all.

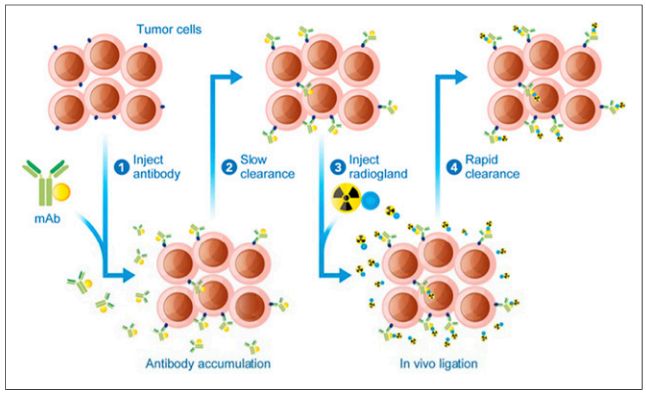

FIGURE 3. Schematic representation of in vivo pretargeting (*42*). mAb = monoclonal antibody.

CONTROLLING THE FATE OF THE DAUGHTERS

On α-emission, recoil energy imparted to the daughter (100 keV) is about 1,000 times higher than the binding energy of any chemical bond, resulting in release of the daughter. Redistribution depends on the distance covered during the recoil process, diffusion processes, and active transport as well as the intrinsic affinity of the radionuclide for certain organs. The time to reach the target and the toxicity to healthy organs are impacted by the $t_{½}$ of the daughter. Redistribution of the recoil progeny is extremely difficult to measure and is performed mostly in postmortem ex vivo analysis of organs.

Redistribution of daughters compromised the continuation of a clinical study using ^{224}Ra; 8% of ^{220}Rn, the gaseous ^{224}Ra daughter, was shown to leave the body, and high uptake of ^{212}Pb and ^{212}Bi was observed in the red blood cells, kidneys (^{212}Bi), and liver (^{212}Pb) (*48*). On the other hand, low redistribution was demonstrated with ^{223}Ra daughters in mice and confirmed in humans (*49*).

Redistribution of ^{213}Bi to the kidneys is a main limitation of ^{225}Ac radiotherapy. Schwartz et al. evaluated the contribution of nonequilibrium ^{213}Bi to kidney dose in mice via γ-ray spectroscopy immediately after tissue harvest and at secular equilibrium (Fig. 4A) (*50*). The average absorbed dose to the kidneys was determined to be 0.77 Gy·kBq^{-1}, of which 60% was attributed to nonequilibrium ^{213}Bi excess (*50*).

The use of α-emitters with a short radioactive $t_{½}$ and simple decay schemes (e.g., ^{213}Bi or ^{211}At) is an effective solution to daughter redistribution. Nevertheless, the higher cytotoxicity of radioisotopes with a longer $t_{½}$ and decay through numerous progeny motivated the development of approaches to control the fate of the daughters. These include a high degree of nanogenerator cellular internalization. High retention of ^{221}Fr and ^{213}Bi inside LNCaP cells was shown in an internalization study with ^{225}Ac-J591. Tumor samples revealed 88% retention of ^{221}Fr and 89% of ^{213}Bi at ^{225}Ac secular equilibrium (Fig. 4B) (*12*).

A second approach relies on the development of a new form of brachytherapy, referred to as diffusing α-emitter radiation therapy. This approach, developed by Arazi et al., involves local administration of wire sources impregnated with radionuclides such as ^{224}Ra in or near the solid tumor tissue (*51*). Necrotic regions of several millimeters were observed around the therapeutic source in several tumor models (Fig. 4C) (*52*). Autoradiography showed a larger distribution around the source for the later decay daughters,

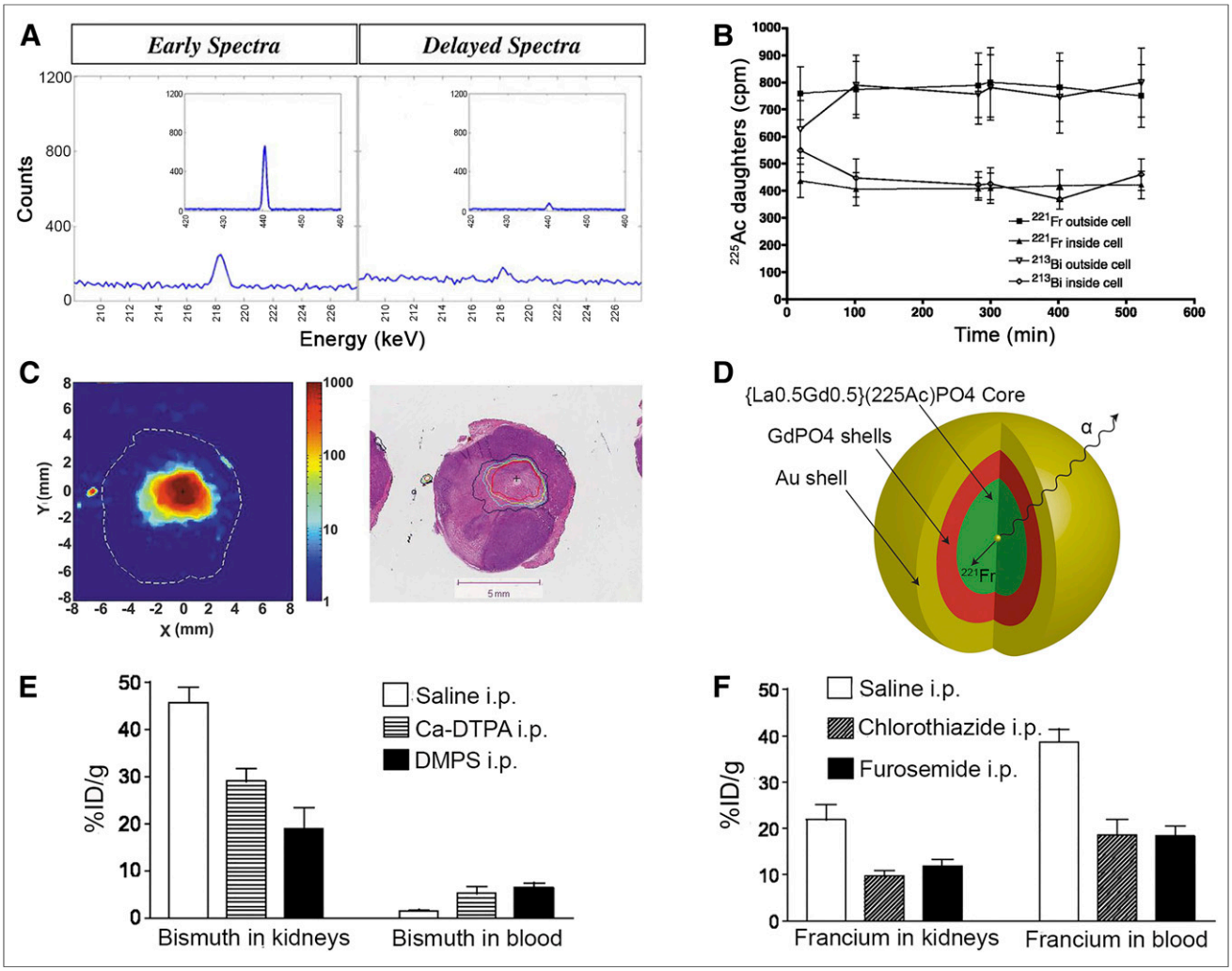

FIGURE 4. Redistribution of α-emitter daughters: approaches to controlling their fate. (A) γ-ray spectroscopy of BALB/C mouse kidneys 96 h after injection of ^{225}Ac-HuM195. Peaks (440 keV) indicate presence of nonequilibrium ^{213}Bi in kidneys. (Reprinted with permission of (*50*).) (B) Internalization and retention of ^{213}Bi and ^{221}Fr daughters in vitro after binding of ^{225}Ac-J591 in LNCaP cells. (Reprinted with permission of (*12*).) (C) High-resolution autoradiography evaluating spread of ^{224}Ra progeny (^{212}Pb) after intratumoral implantation of ^{224}Ra wires in HCT15 tumor model in nude mice. Hematoxylin and eosin staining shows correlation with necrotic domains. (Reprinted with permission of (*52*).) (D) Gold-coated lanthanide phosphate nanoparticle allowing retention of ^{225}Ac and its daughters (*54*). (E) Heavy-metal chelation effect on ^{213}Bi renal uptake 24 h after injection of ^{225}Ac radioimmunotherapy. (F) Furosemide and chlorothiazide effect on ^{221}Fr and ^{212}Bi renal uptake 24 h after injection of ^{225}Ac radioimmunotherapy. %ID = percentage injected dose; DMPS = 2,3-dimercapto-1-propanesulfonic acid; DTPA = diethylenetriaminepentaacetic acid; i.p. = intraperitoneally.

^{212}Bi and ^{212}Pb, compared with the earlier decay daughters, ^{220}Rn and ^{216}Po. Redistribution of ^{212}Pb to the kidneys was observed to be based on tumor size: 90% for 0.1-g tumors but only 12% for 2.4-g tumors (*51*).

Encapsulation of α-emitting radionuclides into nanocarriers was evaluated to retain recoil daughters at the tumor site. ^{223}Ra encapsulation in pegylated liposomal doxorubicin demonstrated sufficient stability in vitro. Skeleton uptake remained lower than for free ^{223}Ra, and higher uptake of the ^{223}Ra daughters, ^{211}Pb and ^{211}Bi, was observed in the kidneys (*53*). ^{225}Ac-doped multishell nanoparticles were evaluated to encapsulate ^{225}Ac and its daughters (Fig. 4D) (*54*). Nanoparticles with 4 $GdPO_4$ shells followed by gold coating demonstrated the greatest retention of ^{255}Ac (>99.99%) and its daughters, with up to 98% of ^{221}Fr retained (*54*).

The use of metal-chelation therapy and diuretics was investigated by Jaggi et al. to reduce renal toxicity during ^{225}Ac radioimmunotherapy (*55*). Dithiols, known to chelate and enhance the urinary excretion of ^{213}Bi, reduced the renal ^{213}Bi activity as early as 6 h after radiotherapy (Fig. 4E) (*55*). An increase in ^{213}Bi blood activity was observed in mice, but this phenomenon was not observed in cynomolgus monkeys (*55*). Furosemide and chlorothiazide, 2 diuretics that inhibit the tubular reabsorption of alkali metals, also significantly reduced ^{221}Fr renal activity (Fig. 4F) (*55*). Though effective with long-circulating biomolecules, such an improvement might not be observed with fast-clearing molecules.

CONCLUSION

The combination of DNA double-strand breaks and indirect cytocidal effects such as cross-fire or radiation-induced bystander effects provides α-particles with exceptional cell-killing potency. Important caveats for the use of α-emitting radionuclides include production and availability limitations, together with redistribution of daughters. Solutions to these issues are currently being investigated and should allow for more widespread development of

α-emitter radiotherapy. Part 2 of this educational review will explore the current preclinical and clinical uses of α-radiotherapy.

REFERENCES

1. Blower PJ. A nuclear chocolate box: the periodic table of nuclear medicine. *Dalton Trans.* 2015;44:4819–4844.
2. Kratochwil C, Bruchertseifer F, Giesel FL, et al. ^{225}Ac-PSMA-617 for PSMA-targeted α-radiation therapy of metastatic castration-resistant prostate cancer. *J Nucl Med.* 2016;57:1941–1944.
3. Baidoo KE, Yong K, Brechbiel MW. Molecular pathways: targeted alpha-particle radiation therapy. *Clin Cancer Res.* 2013;19:530–537.
4. Søyland C, Hassfjell SP. Survival of human lung epithelial cells following in vitro alpha-particle irradiation with absolute determination of the number of alpha-particle traversals of individual cells. *Int J Radiat Biol.* 2000;76:1315–1322.
5. Zhou H, Hong M, Chai Y, Hei TK. Consequences of cytoplasmic irradiation: studies from microbeam. *J Radiat Res (Tokyo).* 2009;50(suppl A):A59–A65.
6. Haberkorn U, Giesel F, Morgenstern A, Kratochwil C. The future of radioligand therapy: alpha, beta or both? *J Nucl Med.* 2017;58:1017–1018.
7. Behling K, Maguire WF, Lopez Puebla JC, et al. Vascular targeted radioimmunotherapy for the treatment of glioblastoma. *J Nucl Med.* 2016;57:1576–1582.
8. Behling K, DiGialleonardo V, Maguire WF, et al. Remodelling the vascular microenvironment of glioblastoma with alpha-particles. *J Nucl Med.* 2016;57:1771–1777.
9. Gorin JB, Menager J, Gouard S, et al. Antitumor immunity induced after alpha irradiation. *Neoplasia.* 2014;16:319–328.
10. Wulbrand C, Seidl C, Gaertner FC, et al. Alpha-particle emitting ^{213}Bi-anti-EGFR immunoconjugates eradicate tumor cells independent of oxygenation. *PLoS One.* 2013;8:e64730.
11. Sgouros G, Roeske JC, McDevitt MR, et al. MIRD pamphlet no. 22 (abridged): radiobiology and dosimetry of alpha-particle emitters for targeted radionuclide therapy. *J Nucl Med.* 2010;51:311–328.
12. McDevitt MR, Ma D, Lai LT, et al. Tumor therapy with targeted atomic nanogenerators. *Science.* 2001;294:1537–1540.
13. Zalutsky MR, Pruszynski M. Astatine-211: production and availability. *Curr Radiopharm.* 2011;4:177–185.
14. Zalutsky MR, Reardon DA, Akabani G, et al. Clinical experience with alpha-particle emitting ^{211}At: treatment of recurrent brain tumor patients with ^{211}At-labeled chimeric antitenascin monoclonal antibody 81C6. *J Nucl Med.* 2008;49:30–38.
15. Vaidyanathan G, Zalutsky MR. Astatine radiopharmaceuticals: prospects and problems. *Curr Radiopharm.* 2008;1:177.
16. Zalutsky MR, Vaidyanathan G. Astatine-211-labeled radiotherapeutics: an emerging approach to targeted alpha-particle radiotherapy. *Curr Pharm Des.* 2000;6:1433–1455.
17. Boll RA, Malkemus D, Mirzadeh S. Production of actinium-225 for alpha particle mediated radioimmunotherapy. *Appl Radiat Isot.* 2005;62:667–679.
18. McDevitt MR, Finn RD, Sgouros G, Ma DS, Scheinberg DA. An Ac-225/Bi-213 generator system for therapeutic clinical applications: construction and operation. *Appl Radiat Isot.* 1999;50:895–904.
19. Griswold JR, Medvedev DG, Engle JW, et al. Large scale accelerator production of ^{225}Ac: effective cross sections for 78-192 MeV protons incident on Th-232 targets. *Appl Radiat Isot.* 2016;118:366–374.
20. Price EW, Orvig C. Matching chelators to radiometals for radiopharmaceuticals. *Chem Soc Rev.* 2014;43:260–290.
21. Deal KA, Davis IA, Mirzadeh S, Kennel SJ, Brechbiel MW. Improved in vivo stability of actinium-225 macrocyclic complexes. *J Med Chem.* 1999;42:2988–2992.
22. Ivanov PI, Collins SM, van Es EM, Garcia-Miranda M, Jerome SM, Russell BC. Evaluation of the separation and purification of Th-227 from its decay progeny by anion exchange and extraction chromatography. *Appl Radiat Isot.* 2017;124:100–105.
23. Henriksen G, Hoff P, Alstad J, Larsen RH. Ra-223 for endoradiotherapeutic applications prepared from an immobilized Ac-227/Th-227 source. *Radiochim Acta.* 2001;89:661–666.
24. Mokhodoeva O, Guseva L, Dogadkin N. Isolation of generator-produced Ra-223 in 0.9-% NaCl solutions containing EDTA for direct radiotherapeutic studies. *J Radioanal Nucl Chem.* 2015;304:449–453.
25. Washiyama K, Amano R, Sasaki J, et al. Th-227-EDTMP: a potential therapeutic agent for bone metastasis. *Nucl Med Biol.* 2004;31:901–908.
26. Dahle J, Borrebaek J, Melhus KB, et al. Initial evaluation of ^{227}Th-p-benzyl-DOTA-rituximab for low-dose rate alpha-particle radioimmunotherapy. *Nucl Med Biol.* 2006;33:271–279.
27. Ramdahl T, Bonge-Hansen HT, Ryan OB, et al. An efficient chelator for complexation of thorium-227. *Bioorg Med Chem Lett.* 2016;26:4318–4321.
28. Hassfjell S. ^{212}Pb generator based on a ^{228}Th source. *Appl Radiat Isot.* 2001;55:433–439.
29. Baidoo KE, Milenic DE, Brechbiel MW. Methodology for labeling proteins and peptides with lead-212. *Nucl Med Biol.* 2013;40:592–599.
30. Wick RR, Chmelevsky D, Gossner W. ^{224}Ra: risk to bone and haematopoietic tissue in ankylosing spondylitis patients. *Strahlentherapie [Sonderb].* 1985;80:38–44.
31. Chappell LL, Dadachova E, Milenic DE, Garmestani K, Wu CC, Brechbiel MW. Synthesis, characterization, and evaluation of a novel bifunctional chelating agent for the lead isotopes Pb-203 and Pb-212. *Nucl Med Biol.* 2000;27:93–100.
32. Yong K, Brechbiel MW. Towards translation of ^{212}Pb as a clinical therapeutic: getting the lead in! *Dalton Trans.* 2011;40:6068–6076.
33. Fremlin J. *Health Risks of Radon and Other Internally Deposited Alpha-Emitters: BEIR-IV.* Washington, DC: National Academies Press; 1988:125–126.
34. Li H, Gu YP, Miki J, et al. Malignant transformation of human benign prostate epithelial cells by high LET alpha-particles. *Int J Oncol.* 2007;31:537–544.
35. Zhou H, Suzuki M, Randers-Pehrson G, et al. Radiation risk to low fluences of alpha particles may be greater than we thought. *Proc Natl Acad Sci USA.* 2001;98:14410–14415.
36. Bosley RB, Simpson JA. Choice of alpha-probe operating voltage to suit a wide range of conditions. *J Radiol Prot.* 2002;22:293–303.
37. Dauer LT, Williamson MJ, Humm J, et al. Radiation safety considerations for the use of $^{223}RaCl_2$ in men with castration-resistant prostate cancer. *Health Phys.* 2014;106:494–504.
38. Tagawa ST, Akhtar NH, Osborne J, et al. Phase II trial of ^{177}lutetium radiolabeled anti-PSMA antibody J591 (Lu-177-J591) for metastatic castrate-resistant prostate cancer (metCRPC): survival update and expansion cohort with biomarkers [abstract]. *J Clin Oncol.* 2013;31(suppl):121.
39. Guérard F, Gestin JF, Brechbiel MW. Production of [At-211]-astatinated radiopharmaceuticals and applications in targeted alpha-particle therapy. *Cancer Biother Radiopharm.* 2013;28:1–20.
40. McDevitt MR, Ma D, Simon J, Frank RK, Scheinberg DA. Design and synthesis of ^{225}Ac radioimmunopharmaceuticals. *Appl Radiat Isot.* 2002;57:841–847.
41. Maguire WF, McDevitt MR, Smith-Jones PM, Scheinberg DA. Efficient 1-step radiolabeling of monoclonal antibodies to high specific activity with ^{225}Ac for alpha-particle radioimmunotherapy of cancer. *J Nucl Med.* 2014;55:1492–1498.
42. Altai M, Membreno R, Cook B, Tolmachev V, Zeglis B. Pretargeted imaging and therapy. *J Nucl Med.* 2017;58:1553–1559.
43. Lesch HP, Kaikkonen MU, Pikkarainen JT, Yla-Herttuala S. Avidin-biotin technology in targeted therapy. *Expert Opin Drug Deliv.* 2010;7:551–564.
44. Goldenberg DM, Chatal JF, Barbet J, Boerman O, Sharkey RM. Cancer imaging and therapy with bispecific antibody pretargeting. *Update Cancer Ther.* 2007;2:19–31.
45. Knight JC, Cornelissen B. Bioorthogonal chemistry: implications for pretargeted nuclear (PET/SPECT) imaging and therapy. *Am J Nucl Med Mol Imaging.* 2014;4:96–113.
46. Frost SH, Back T, Chouin N, et al. Comparison of ^{211}At-PRIT and ^{211}At-RIT of ovarian microtumors in a nude mouse model. *Cancer Biother Radiopharm.* 2013;28:108–114.
47. Yao Z, Zhang M, Garmestani K, et al. Pretargeted alpha emitting radioimmunotherapy using ^{213}Bi 1,4,7,10-tetraazacyclododecane-*N,N′,N′′,N′′′*-tetraacetic acid-biotin. *Clin Cancer Res.* 2004;10:3137–3146.
48. Lloyd RD, Mays CW, Taylor GN, Atherton DR, Bruenger FW, Jones CW. Radium-224 retention, distribution, and dosimetry in beagles. *Radiat Res.* 1982;92:280–295.
49. Carrasquillo JA, O'Donoghue JA, Pandit-Taskar N, et al. Phase I pharmacokinetic and biodistribution study with escalating doses of ^{223}Ra-dichloride in men with castration-resistant metastatic prostate cancer. *Eur J Nucl Med Mol Imaging.* 2013;40:1384–1393.
50. Schwartz J, Jaggi JS, O'Donoghue JA, et al. Renal uptake of bismuth-213 and its contribution to kidney radiation dose following administration of actinium-225-labeled antibody. *Phys Med Biol.* 2011;56:721–733.
51. Arazi L, Cooks T, Schmidt M, Keisari Y, Kelson I. Treatment of solid tumors by interstitial release of recoiling short-lived alpha emitters. *Phys Med Biol.* 2007;52:5025–5042.
52. Cooks T, Tal M, Raab S, et al. Intratumoral ^{224}Ra-loaded wires spread alpha-emitters inside solid human tumors in athymic mice achieving tumor control. *Anticancer Res.* 2012;32:5315–5321.
53. Jonasdottir TJ, Fisher DR, Borrebaek J, Bruland OS, Larsen RH. First in vivo evaluation of liposome-encapsulated ^{223}Ra as a potential alpha-particle-emitting cancer therapeutic agent. *Anticancer Res.* 2006;26:2841–2848.
54. McLaughlin MF, Woodward J, Boll RA, et al. Gold coated lanthanide phosphate nanoparticles for targeted alpha generator radiotherapy. *PLoS One.* 2013;8:e54531.
55. Jaggi JS, Kappel BJ, McDevitt MR, et al. Efforts to control the errant products of a targeted in vivo generator. *Cancer Res.* 2005;65:4888–4895.
56. Miederer M, Scheinberg DA, McDevitt MR. Realizing the potential of the actinium-225 radionuclide generator in targeted alpha particle therapy applications. *Adv Drug Deliv Rev.* 2008;60:1371–1382.
57. Larsen RH, Saxtorph H, Skydsgaard M, et al. Radiotoxicity of the alpha-emitting bone-seeker ^{223}Ra injected intravenously into mice: histology, clinical chemistry and hematology. *In Vivo.* 2006;20:325–331.
58. de Kruijff RM, Wolterbeek HT, Denkova AG. A critical review of alpha radionuclide therapy-how to deal with recoiling daughters? *Pharmaceuticals (Basel).* 2015;8:321–336.